Three-dimensional mapping reveals scale-dependent dynamics in biogenic reef habitat structure

Jackson-Bué, Tim; Williams, Gareth; Walker-Springett, Guy; Rowlands, Steven; Davies, Andrew

Remote Sensing in Ecology and Conservation

DOI:
10.1002/rse2.213

E-pub ahead of print: 15/05/2021

Peer reviewed version

Three-dimensional mapping reveals scale-dependent dynamics in biogenic reef habitat structure

Tim Jackson-Bué[1*], Gareth J. Williams[1], Guy Walker-Springett[1], Steven J. Rowlands[1], Andrew J. Davies[2]

[1]School of Ocean Sciences, Bangor University, Anglesey LL59 5AB, UK

[2]Department of Biological Sciences, University of Rhode Island, Kingston, RI, USA

*Corresponding author

Email: t.d.jackson@bangor.ac.uk

Tel: +44 (0) 7841463590

Orchid IDs:

TJB 0000-0001-7077-2186

GJW 0000-0001-7837-1619

GWS 0000-0002-4544-7573

SJR 0000-0002-7969-3705

AJD 0000-0002-2087-0885

Running Title

Scale-dependent biogenic reef dynamics

Word count

Abstract: 290

Main text: 5139

Acknowledgements: 111

References: 2179

Table and figure legends: 953

Tables: 0

Figures: 7

Abstract

Habitat structure influences a broad range of ecological interactions and ecosystem functions across biomes. To understand and effectively manage dynamic ecosystems, we need detailed information about habitat properties and how they vary across spatial and temporal scales. Measuring and monitoring variation in three-dimensional (3D) habitat structure has traditionally been challenging, despite recognition of its importance to ecological processes. Modern 3D mapping technologies present opportunities to characterise spatial and temporal variation in habitat structure at a range of ecologically relevant scales. Biogenic reefs are structurally complex and dynamic habitats, in which structure has a pivotal influence on ecosystem biodiversity, function and resilience. For the first time, we characterised spatial and temporal dynamics in the 3D structure of intertidal *Sabellaria alveolata* biogenic reef across scales. We used drone-derived structure-from-motion photogrammetry and terrestrial laser scanning to characterise reef structural variation at mm to cm resolutions at a habitat scale (~35,000 m^2) over one year, and at a plot scale (2,500 m^2) over five years (2014-2019, 6-month intervals). We found that most of the variation in reef emergence above the substrate, accretion rate and erosion rate was explained by a combination of systematic trends with shore height and positive spatial autocorrelation up to the scale of colonies (1.5 m) or small patches (up to 4 m). We identified previously undocumented temporal patterns in intertidal *S. alveolata* reef accretion and erosion, specifically groups of rapidly accreting, short-lived colonies and slow accreting, long-lived colonies. We showed that these highly dynamic colony-scale structural changes compensate for each other, resulting in seemingly stable reef habitat structure over larger spatial and temporal scales. These patterns could only be detected with the use of modern 3D mapping technologies, demonstrating their potential to enhance our understanding of ecosystem dynamics across scales.

Keywords

autocorrelation, ecosystem dynamics, reef accretion, reef erosion, reef mapping, spatial ecology

Introduction

Ecosystems are dynamic (Odum, 1969). Gradients in biophysical and human socioeconomic drivers create complex mosaics in ecosystem properties (Legendre and Fortin, 1989; Perry, 2002; Williams et al., 2019), with the patterns we observe determined by the scale of our observations (Levin, 1992; Wiens, 1989). Because ecosystem patterns and processes are intrinsically linked, we can gain a deeper understanding about ecological processes and their drivers by quantifying these underlying patterns across scales (Horne and Schneider, 1995; Underwood et al., 2000). Quantifying patterns in ecosystem properties not only advances ecological insight, but also facilitates evidence-based management by enabling us to detect change in ecosystem characteristics like habitat structure in response to disturbance (Landres et al., 1999).

Physical habitat structure can be abiotic like rocks on a shoreline, or biogenic like the trees of a forest. These features determine habitat structural complexity and influence the biodiversity and community composition of associated ecological communities through myriad processes. These include buffering organisms from extreme environmental conditions (Scheffers et al., 2014), mediating resource availability (Safriel and Ben-Eliahu, 1991), and providing shelter for prey species from predation (Stevenson et al., 2015; Warfe et al., 2008). Biogenic reefs are complex habitats in which substrate and structure is generated and amplified by engineering organisms (Jones et al., 1994). Biogenic reefs represent global biodiversity hotspots and provide a range of ecosystem services to humanity (Bruschetti, 2019; Connell, 1978; Dubois et al., 2002; Woodhead et al., 2019). Spatially and temporally dynamic three-dimensional (3D) structure is critical to the biodiversity, ecological functioning and conservation value of biogenic reefs (Graham and Nash, 2013; Holt et al., 1998). Metrics of reef structure can also be an indicator of the health of the engineering species (Curd et al., 2019) and reef recovery potential following acute disturbance (Graham et al., 2015). To understand organism-habitat interactions within biogenic reef systems, we must first identify the patterns and scales of variation inherent within their structures (Holt et al., 1998; Jenkins et al., 2018).

Much of our understanding about scale-dependent processes in ecosystems derives from terrestrial landscape ecology. The study of spatial patterns in terrestrial systems has greatly benefitted from remote sensing, providing high-resolution, spatially continuous data for a variety of ecosystem properties including 3D habitat structure (Chambers et al., 2007; Vierling et al., 2008). Remote sensing of 3D structure in the marine environment from satellite or crewed aircraft improves ecological insight in clear, shallow waters (Wedding et al., 2019), but similar information is challenging and expensive to capture in deep or turbid waters (Lecours et al., 2015). Recent developments in high-resolution 3D mapping technologies including structure-from-motion photogrammetry and laser scanning offer the potential to study patterns in 3D structure from organism

to habitat scales, and are practical for investigation of scale-dependent properties in marine and coastal habitats (Calders et al., 2020; Urbina-Barreto et al., 2021). This creates opportunities to apply conceptual and analytical frameworks from landscape ecology, such as identification of dominant spatial scales of variation (Legendre and Fortin, 1989), at new scales and in new systems. The ability to record spatially continuous 3D habitat structure across km-extents at mm resolution, with rapid repeats and low operating costs is sparking a revolution in the scope and scale of ecological investigations (D'Urban Jackson et al., 2020).

Here we use intertidal habitat structure built by *Sabellaria alveolata,* a reef-building annelid, as a model system to characterise scale-dependent structural dynamics in complex biogenic reef habitats using high-resolution 3D mapping. *S. alveolata* reef comprises colonies of sediment tubes biocemented together, creating extensive reefs on northeast Atlantic and Mediterranean coasts (Bruschetti, 2019; Godet et al., 2011; La Porta and Nicoletti, 2009). Similar reefs built by other species in the Sabellariidae family are found globally (Capa et al., 2012). Our current understanding of the scale-dependent structural dynamics in biogenic reefs is hampered by a lack of spatio-temporal information about habitat structure across scales. To explore this, we quantify spatial and temporal patterns in reef structure at mm to cm resolution, at plot- (2,500 m^2) to habitat-scale (~35,000 m^2) extents and over temporal scales of 1-5 years. Our findings reveal previously undescribed patterns of structural variation in intertidal biogenic reefs and demonstrate the enhanced ecological insight gained from the application of modern remote sensing technologies for 3D ecosystem mapping in structurally complex habitats.

Methods

Data collection

Study site

To characterise variation in biogenic reef habitat structure across scales we conducted high-resolution 3D mapping at a *Sabellaria alveolata* reef habitat at Llanddulas, Wales, UK (53.294 N, 3.632 W) using two techniques between 2014 and 2019 (Fig. 1). The reef at Llanddulas occupies the low shore for at least one kilometre along a moderately exposed, unconsolidated cobble beach with a gentle slope gradient of 3%.

Plot-scale (2,500 m^2) 3D mapping

We collected data to investigate multi-annual temporal patterns in *S. alveolata* reef structure using terrestrial laser scanning (HDS ScanStation C10, Leica Geosystems, Switzerland) of a permanent 2,500 m^2 reef plot at approximately 6-month intervals (autumn and spring) over 5 years from September 2014 to October 2019. Terrestrial laser scanning generates high-resolution (thousands of points per m^2) data with mm precision and was the most advanced 3D mapping technology available for field sampling at the start of the study in 2014. We conducted medium resolution (0.1 m point spacing at 100 m range) scans of the plot from several stationary positions per time point, ensuring similar data coverage among time points. We used retroreflective sphere reference targets to align scan datasets within a time point. Aligning datasets from different time points typically uses global navigation satellite system (GNSS) georeferencing or permanent reference targets. Our plot was intertidal with an unconsolidated substrate, so permanent targets could not be left and expected not to move, and alignment by GNSS georeferencing would have introduced error on the same scale (cm) as the changes we expected to detect, limiting their reliable detection and interpretation. Therefore, to enable accurate alignment of repeat surveys we increased the laser scanning data coverage to include permanent nearby features (rock groynes, cycle path and buildings), enabling us to align the datasets using the geometry of these stable features, without constraining the data across the dynamic foreshore.

We quality checked, aligned, georeferenced and manually cleaned the laser scanning point cloud data in Cyclone v9 software (Leica Geosystems, Switzerland). Within a time point, we aligned datasets from different scanner positions to 6 mm accuracy using target positions. We then aligned complete datasets from different time points to 6 mm accuracy using the geometry of permanent features. We made a final adjustment to the vertical alignment within the plot based on stable regions of non-reef

substrate. We standardised datasets from different time points by cropping to the plot extent, subsampling point clouds to a minimum point spacing of 5 mm, and removing isolated points using the *statistical outlier removal* tool in the open source software CloudCompare v2.11 (CloudCompare, 2019).

Habitat-scale (~35,000 m^2) 3D mapping

Terrestrial laser scanning was impractical for the larger extent of habitat-scale sampling within short low-tide windows. Therefore, to investigate spatial and temporal patterns in *S. alveolata* reef structure at a habitat scale (~35,000 m^2) we used structure-from-motion photogrammetry derived from drone aerial imagery, in April 2018 and April 2019. Drone-derived structure-from-motion photogrammetry generates continuous 3D information across large extents, with comparable accuracy to terrestrial laser scanning in complex habitats like *S. alveolata* reef (D'Urban Jackson et al., 2020). We used a Phantom 4 Pro (DJI) with a 20 MP camera flying at 46 m altitude to capture images with 14 mm XY ground resolution, covering approximately 150,000 m^2 of the coastline. The flight pattern was pre-determined and flying was automated using software (Maps Made Easy) to ensure the same survey pattern was flown in both years. To optimise the 3D modelling process, we used a high image overlap, so that every XY position in the area of interest was captured in at least 5 images. We generated 3D models for each survey using the industry standard software Pix4Dmapper Pro v4. Unlike terrestrial laser scanning, for structure-from-motion photogrammetry we required georeferenced ground control points to scale, constrain and align the 3D models. We used 11 (2018) and 19 (2019) control points surveyed with commercial GNSS equipment (system 1200, Leica Geosystems, Switzerland), giving root mean square errors of 9 mm and 32 mm respectively. Because there were no permanent features within the study area, we verified vertical alignment accuracy by calculating elevation difference at 100 random points along a cycle path adjacent to the study area, giving a median difference of 23 mm and root mean square error of 26 mm. This represents a worst-case estimate because the cycle path was outside the area constrained by control points. From the 3D models and aerial images, we generated digital surface models (DSMs, 0.1 m XY resolution) and orthomosaics (0.02 m XY resolution) for 2018 and 2019.

Data analysis

Habitat-scale (~35,000 m^2) spatial patterns in S. alveolata *reef emergence, accretion rate and erosion rate*

To study habitat-scale spatial patterns of variation in *S. alveolata* reef structure we conducted variography (Fig. 2, Supporting information) using the drone-derived digital surface models (DSMs) from 2018 and 2019. To investigate reef structure independently from trends in the underlying non-reef substrate, we calculated reef *emergence*, defined as the height of the DSM surfaces above a standardised digital elevation model (DEM) representing the lowest levels in the non-reef substrate (Fig. 3). We used a threshold of emergence to classify DSM cells as reef (≥ 0.15 m) or non-reef substrate (< 0.15 m) within a *reef area* polygon (36,363 m^2) digitised from the 2018 orthomosaic. We validated the classification by manually classifying 500 random points on the orthomosaic and interpreting a confusion matrix of predicted against observed classes. Overall accuracy (correct predictions out of total predictions) was 81.2%, precisions (true positives out of total positive predictions) were 91.7% and 80.1% for reef and non-reef substrate, respectively. To study spatial patterns in accretion (positive change) and erosion (negative change) of *S. alveolata* reef we calculated the vertical difference between the DSMs from April 2018 and April 2019, to provide accretion and erosion rates as positive and negative vertical change per year.

To characterise spatial variation in habitat-scale *S. alveolata* reef structure, we modelled trends and conducted variography using emergence, accretion rate and erosion rate values of the 9140 reef cells in a random sample of 100,000 cells in the reef area. Our data exploration indicated that emergence, accretion rate and erosion rate had trends with shore height and along-shore distance and were anisotropic with a major axis along the shore and minor axis down the shore. To meet the gaussian distribution requirements of linear modelling and variography, we transformed the data using ordered quantile transformation (Peterson and Cavanaugh, 2020), then modelled trends using ordinary least squares linear regression. We conducted variography on the linear model residuals along two axes: along the shore (120° from north) and down the shore (30° from north), with maximum lags of 250 m and 50 m respectively, approximately two thirds of the maximum reef area dimensions, using the *gstat* package in R (Graler et al., 2016; Pebesma, 2004; R Core Team, 2020). We fitted an initial variogram model to each experimental variogram automatically, then improved the fit by adjusting the model parameters and adding a secondary variogram model where appropriate, until a visual good fit was found to the experimental variogram (Gringarten and Deutsch, 2001). To investigate whether patterns in reef structure were related directly to patterns in the underlying non-reef substrate

topography we conducted variography using emergence data from 10,000 random non-reef substrate DSM cells.

The trend in mean emergence with shore height explained only a small amount of the variation (R^2 = 0.043, Supporting information table S1). Our data exploration showed that the reef comprised colonies at all stages of emergence, from the classification threshold of 0.15 m up to an emergence limit that was related to shore height. Therefore, shore height appeared to represent a limiting factor and so maximum emergence was a better metric for characterising habitat structure than a measure of central tendency (Kaiser et al., 1994). To examine the relationship between maximum reef emergence and shore height we used a sample of 2,000 reef cells with a minimum point spacing of 1.5 m derived from the variography results, 1.5 m being the dominant range of spatial autocorrelation. We modelled the relationship between maximum (99th percentile) reef emergence and DEM elevation with linear quantile regression, using the *quantreg* package in R (Koenker, 2020).

Plot-scale (2,500 m^2) temporal patterns in reef structure

To characterise multi-annual structural changes in *S. alveolata* reef structure, we used terrestrial laser scanning to survey a 2,500 m^2 plot in autumn and spring from September 2014 to October 2019. To track vertical changes in reef emergence through time we digitally sampled locations within the plot (n = 454) that had reef presence in at least one time point, avoided reef colony edges where lateral accretion and erosion would confuse interpretation, and were spatially independent (Fig. 4, Supporting information). At each sample location and for each time point, we extracted mean emergence above a common DEM. To examine common characteristics in temporal changes in reef emergence, we derived accretion and emergence metrics from each sample timeseries. We calculated mean and maximum annual accretion rate, maximum emergence, and time spent within 80% of maximum emergence, which we termed *persistence*. We then used partitioning around medoids (PAM) clustering, a common data clustering method that is robust to outliers (Kaufman and Rousseeuw, 1990), to classify sample timeseries' into two groups with similar metrics using the *cluster* package in R (Maechler et al., 2019).

Following evidence of multiannual cycles of habitat-scale accretion and erosion (Gruet, 1986), we hypothesised that mean plot-scale reef emergence would vary over the 5 year study period. We also hypothesised that due to higher productivity in summer and lower growth rates coupled with more destructive wave action in winter, plot-scale emergence would be higher in autumn than in spring. We tested these hypotheses using a two fixed-factor (year and season) permutational analysis of variance (Anderson, 2001) with reef emergence as a univariate response. The permutational nature of the test removes the need to satisfy normality in the response variable as the routine permutes the raw data to

generate the null distribution (Anderson, 2001). To ensure a balanced design with no missing data and no repeat sampling, we first divided reef sample locations (n = 454) randomly and equally among season (2 levels: autumn and spring) and year (5 levels: 2015-2019) combinations (10 combinations, n = 45). Some reef sample locations contained missing data for certain season and year combinations, so we iteratively exchanged these reef sample locations among groups until no missing data remained. Homogeneity of variance between factor levels was confirmed with Levene's test ($P > 0.05$). Our permutational analysis of variance was based on a Euclidean distance similarity matrix of the raw reef emergence data, with 9999 random permutations under a reduced model and Type III (partial) sums of squares. Where there was global model significance, permutational pairwise tests were used to determine where the differences occurred between factor levels.

Results

Habitat-scale (~35,000 m^2) spatial patterns in S. alveolata *reef emergence, accretion rate and erosion rate*

We estimated the percentage cover of *S. alveolata* reef within the 36,363 m^2 reef area as 26.8% or a total coverage of 9,745 m^2 based on our binary classification of the 0.1 m XY resolution emergence raster into reef or non-reef substrate (Fig. 5A). Maximum reef emergence (99th percentile) increased down the shore from approximately 0.2 m at 0 m ordnance datum Newlyn (ODN) to a maximum of 0.5 m above the substrate at 2.8 m below ODN (Fig. 5B). The relationship was described by:

$$\log(emergence_{max}) = -0.308(shore\ height) - 1.551 \quad (1)$$

Reef emergence was positively spatially autocorrelated up to 1.5 m in both along shore and down shore directions, represented by a spatial structure that described 65-70% of the variance (Fig. 5C, Supporting information table S1.). There was a smaller amount of residual positive autocorrelation in reef emergence over larger distances along the shore (up to 110 m) and down the shore (up to 20 m) (Fig. 5C, Supporting information table S1). At larger distances still, the variogram indicated additional patterns in spatial dependence of reef emergence including cyclicity, but these were not quantified because variogram model fitting becomes less reliable at larger distances relative to the study extent. The variogram of non-reef substrate emergence showed that the dominant autocorrelation pattern mostly occurred over a larger distance of 4.5 m and explained a higher proportion (90%) of the variation compared to reef emergence (Supporting information table S1). A small amount of spatial autocorrelation in non-reef substrate emergence was also evident over larger distances (up to 50 – 90 m).

At the habitat scale (~35,000 m^2), the elevation of *S. alveolata* reef colonies changed by 19 ± 82 mm (mean ± 1 sd) between April 2018 and April 2019 (Fig. 6A). The small magnitude of mean elevation change across the total reef area was the result of a balance between variable positive and negative changes of individual samples (0.1 m XY resolution cells). A high proportion of reef samples (80%) showed a small positive elevation change (accretion, 49 ± 30 mm), with the remaining samples (20%) showing larger and more variable negative changes (erosion, -99 ± 113 mm). Both accretion and erosion maxima increased towards the lower shore (Fig. 6A) and showed different spatial autocorrelation patterns. Positive spatial autocorrelation in accretion mostly occurred within short distances (up to 0.75 – 1.05 m), with a small proportion of positive autocorrelation extending over larger distances up to 40-130 m (Fig. 6B, Supporting information table S2). In contrast, erosion of

reef material was only positively spatially autocorrelated up to distances of 2.9 – 3.8 m, beyond which the variogram indicated spatial randomness (Fig. 6C, Supporting information table S2).

Plot-scale (2,500 m^2) temporal patterns in reef structure

Within the 2,500 m^2 plot, overall reef emergence across all 11 time points over 5 years was 0.22 ± 0.13 m (mean ± 1 sd). We found scale dependent variation, with high variation in emergence at each sample location (colony-scale, n = 454) through time and high variation among samples at each time point, but low variation in plot-scale emergence through time. The coefficient of variation (mean ± 1 sd) in sample location emergence through time was 52 ± 32.3, and per time point was 56.5 ± 3.7, whereas the coefficient of variation in plot-scale mean emergence through time was 8.8.

Timeseries' of emergence at reef sample locations revealed diverse temporal patterns in emergence, accretion, and erosion metrics of colonies, that we classified into two groups called *fast* and *slow* colonies (Fig. 7). These two groups clustered moderately well, indicated by an average silhouette width of 0.35 on a scale from 0 (poorly clustered) to 1 (perfectly clustered) (Kaufman and Rousseeuw, 1990). Fast colonies were characterised by higher maximum and mean annual accretion, higher maximum emergence and shorter persistence (time spent within 80% of their maximum emergence) than slow colonies (Fig. 7, Supporting information table S3). Visual assessment showed that slow colonies were evenly distributed throughout the plot, whereas fast colonies were concentrated in the northern, lower-shore half of the plot (Supporting information figure S1). We found that erosion of reef colonies often occurred rapidly in both groups; it was common for emergence to drop to the level of the non-reef substrate within 6 months to a year (Fig. 7).

There was a significant interaction between 'year' and 'season' on plot-scale reef emergence ($F_{4,440}$ = 3.48, P = 0.009, Supporting information table S4) driven entirely by emergence being higher in autumn than spring in 2015 (P = 0.001). Across season, there were no differences among years in spring emergence, but there were significant differences in autumn, with 2015, 2016 and 2019 having higher emergence than 2017 and 2018 (P < 0.05, Supporting information figure S2, Supporting information table S4).

Discussion

Habitat structure strongly dictates ecological function in complex 3D ecosystems. Quantifying how 3D habitat structure varies across space and time is therefore a crucial step in understanding ecosystem dynamics and guiding their effective management. Here, for the first time, we quantified patterns of spatial and temporal variation in 3D habitat structure across scales in an ecologically important but understudied *Sabellaria alveolata* biogenic reef habitat. Our results reveal that patterns in reef emergence, accretion rate and erosion rate are spatially autocorrelated and highly scale-dependent. In this system, reef colonies formed groups of rapidly accreting short-lived colonies and slow accreting long-lived colonies, creating dynamic structure at fine spatial (m) and temporal (6 month) scales. However, these colony-scale dynamics cancel each other out at larger spatial (50m – 1 km) and temporal (5 year) scales, resulting in seemingly stable reef habitat (Fig. 7). This habitat steady-state despite the mosaic of small-scale dynamics is akin to other biogenic systems like forests, where scale-dependent patterns in ecosystem properties have been better studied using remote sensing (Chambers et al., 2013). Using modern 3D mapping we have quantified spatially continuous, cross-scale habitat structure in a biogenic reef, revealing scale-dependent patterns that indicate parallels in structural dynamics between terrestrial and marine biogenic habitats.

Spatial patterns in reef habitat structure

We identified predictable trends in maximum reef emergence, accretion rate and erosion rate, that all increased towards the lower shore. Shore height trends are ubiquitous in intertidal ecosystems like rocky shores and saltmarshes because numerous biological, chemical and physical structuring processes correlate with vertical position (Chappuis et al., 2014; Connell, 1972; Pennings and Callaway, 1992). The trends in our data can be explained by spatially varying hydrodynamic forces, proposed as the most important abiotic structuring factor of *S. alveolata* reef habitat (Collin et al., 2018; Gruet, 1986; Wilson, 1971). Wave forces are predicted to be greatest at the lower shore, with energy attenuated as waves travel across the rough reef surface (Bouma et al., 2014; Lowe et al., 2005). We suggest that higher wave energy at the lower shore results in more coarse sediment being resuspended higher in the water column, enabling faster reef colony accretion and higher maximum emergence. Wave energy can also be destructive, increasing reef erosion rate towards the lower shore. In addition, longer periods of immersion experienced lower on the shore give more time for both reef accretion and erosion.

Interactions between individuals can produce spatially coherent self-organised patterns that influence ecosystem-scale processes in many natural systems, including mussel reefs (Van De Koppel et al., 2008) and arid vegetation (Klausmeier, 1999). We found evidence for self-organisation in *S. alveolata*

reef emergence and accretion rate, that were spatially clustered (positively autocorrelated) up to colony scales (1.5 m). Prograding *S. alveolata* reef colonies have characteristic smooth surfaces comprising the openings of dense, parallel tubes (Fig. 1) (Curd et al., 2019; Ventura et al., 2020). To maintain this morphology as the colony grows, within-colony accretion rate and emergence must be similar among worms. Self-organisation enhances habitat resilience (Guichard et al., 2003; Liu et al., 2014), and in this system the colony morphology may contribute to the remarkable wave-resistance in the friable intertidal structures (Le Cam et al., 2011), analogous to massive stony coral morphologies that can dominate wave-exposed subtidal tropical reefs (Chappell, 1980).

Spatial patterns in biogenic reef properties provide insight into the biotic and abiotic drivers of ecosystem structuring processes (Aston et al., 2019; Edwards et al., 2017; Ford et al., 2020). In our system, reef emergence and accretion rates showed secondary spatial clustering at habitat scales (20-40 m down the shore, 110-130 m along the shore), whereas erosion rates showed spatial randomness beyond 4 m. Habitat-scale spatial clustering in reef emergence and accretion rate may be due to spatial variation in resources (e.g., sediment or food quality), environmental conditions (e.g., salinity), biotic factors (e.g., recruitment density) or anthropogenic influence (e.g., trampling). Interactions between myriad drivers are likely to influence reef structure at various scales (Collin et al., 2018). Identification of the relative importance of these factors and how they vary in time and space warrants further investigation, and may help explain why *S. alveolata* reef structure is highly variable among sites (Stone et al., 2019). Spatial clustering of erosion rates up to 4 m indicates that erosion mostly occurs as the catastrophic collapse of entire *S. alveolata* colonies and platform sections. The lack of larger scale spatial autocorrelation in erosion rates shows that colony collapse is random after accounting for shore height trends, suggesting that destructive processes are similar horizontally along the shore.

Modern remote sensing technologies are advancing our ability to describe and interrogate spatial patterns in marine reef systems. In intertidal habitats like *S. alveolata* reef, aerial methods can capture a range of ecologically relevant information at high resolution across large extents of several km^2 (Bajjouk et al., 2020; Collin et al., 2019, 2018). The importance of 3D ecosystem structure in ecological investigations is recognised, and tools to capture and analyse 3D structure in diverse systems including subtidal reefs are becoming increasingly powerful and accessible (D'Urban Jackson et al., 2020; Lepczyk et al., 2021).

Temporal patterns in biogenic reef structure

Identifying key scales of variation and their forcing processes has been a persistent challenge in ecology (Chave, 2013; Denny et al., 2004; Levin, 1992), especially in marine systems beyond the observation capabilities of traditional remote sensing (Lecours et al., 2015; Wedding et al., 2011). Our

study reveals previously undescribed patterns of scale-dependent spatio-temporal variation in *S. alveolata* reef structure. We found that individual *S. alveolata* colonies on the scale of metres undergo independent and compensatory accretion and erosion cycles, resulting in stability at larger spatial (2,500 m^2) and temporal (5 year) scales. Previous characterisation of *S. alveolata* reef structural dynamics have described multiannual accretion and erosion cycles operating over large areas of reef (10s – 100s m) at some sites, and multiannual stability at others (Gruet, 1986; Lecornu et al., 2016). While we recorded stability in reef structure over a period of 5 years, at decadal time scales the habitat can be transient (Firth et al., 2015). Scale-dependent structural dynamism is a feature of other systems like terrestrial forests (Chambers et al., 2013), and our results indicate that conceptual frameworks from terrestrial landscape ecology can be applied to biogenic reef systems. For instance, the stability of a forest ecosystem can be modelled as a product of the spatial and temporal scales of disturbance events that it experiences (Turner et al., 1993). Applying this concept to our study system, disturbance events (colony collapse) were small in size (up to 4 m) relative to the habitat size (~35,000 m^2) and disturbance (collapse) intervals were generally longer than recovery (accretion to maximum emergence) intervals. As predicted by the conceptual model (Turner et al., 1993), we observed stability in the system at the habitat scale.

We identified two distinct types of reef colonies: "fast" colonies with rapid accretion, high maximum emergence, and short lifespan, and "slow" colonies with slower accretion, lower maximum emergence and longer lifespan. Accretion rates of "fast" *S. alveolata* colonies in our study (mean 0.109 m yr^{-1}, max 0.215 m yr^{-1}) were comparable to upper estimates of 0.105 m yr^{-1} in Cornwall, UK, and >0.5 m yr^{-1} in Normandy, France (Gruet, 1986; Wilson, 1971). These studies documented faster accretion rates in new, small colonies and a similar general pattern could be seen in our timeseries', although variation was high and many colonies had incomplete structural cycles within our study period. We found new, low emergent colonies accreted rapidly and then accretion slowed as they approached a maximum emergence, followed by a period of persistence at the maximum emergence and eventual rapid collapse. A similar accretion pattern has been documented in oyster (*Crassostrea virginica*) reefs, with rapid accretion in deeper edges of a reef (8 m diameter) while no change was recorded in the shallowest central portions, just 2 m away (Rodriguez et al., 2014). This fine-scale spatial variation in structural characteristics would be lost at larger observational scales, highlighting the need for a multiscale approach when assessing the resilience of biogenic reefs to pressures like sea level rise.

Seasonal patterns of accretion and erosion in *S. alveolata* reef and their driving processes are not well understood. We did not find evidence for a consistent seasonal pattern in reef emergence, and while reef emergence measured in autumn showed some variation, spring observations were stable over 5 years (Supporting information figure S2, Supporting information table S4). However, we did find a seasonal difference in one survey year (2015). Temperature and wave energy are two dominant

seasonally varying factors in intertidal habitats. The habitat is vulnerable to severe winter temperatures and damage from winter storms (Crisp, 1964; Firth et al., 2015). In summer, higher temperatures and increased food availability in summer may promote worm productivity that translates to increased accretion rate, but the availability of resuspended sediment with low summer wave action may limit accretion rate. Hydrodynamic energy promotes both *S. alveolata* reef accretion and erosion, so the effects of seasonal variation in wave energy are difficult to predict. Higher emergence in the autumn of 2015 compared to the spring appeared to be a result of heavy recruitment during the summer of that year (TDJ, *pers. obs.*), resulting in many new, rapidly accreting colonies. Recruitment of pelagic larvae to *S. alveolata* reefs is through a combination of continuous low-level settlement and stochastic heavy settlement events when hydrodynamic conditions are favourable (Ayata et al., 2009; Bush et al., 2015; Dubois et al., 2007). Sabellariid worms respond to storm damage with increased reproductive output in a similar way that some plants respond to fire (Barry, 1989) and *S. alveolata* larvae show high levels of retention within local geographic areas (Bush et al., 2015; Dubois et al., 2007). These factors likely result in compensatory self-recruitment to a damaged reef, contributing to long term reef persistence.

Conclusion

Our findings represent the most comprehensive characterisation of *S. alveolata* biogenic reef habitat structure across spatial and temporal scales to date, expanding our understanding of scale-dependent structural dynamics in this complex 3D habitat. We found that *S. alveolata* reef structure is characterised by a mosaic of different colony successional states leading to a dynamic landscape at smaller scales (m), while displaying relative stability (a steady state) at larger spatial and temporal scales. This phenomenon is characteristic of other structurally complex ecosystems like forests and we hypothesise could be true for other colonial reef systems, such as subtidal tropical coral reefs. We also identified previously undocumented temporal patterns in reef structure, specifically distinct groups of “fast and “slow” colonies. The patterns we documented could only be detected with high-resolution 3D mapping, demonstrating the enhanced ecological insight gained from the adoption of contemporary technologies in modern ecology. Scale-dependent ecosystem patterns have historically been challenging to study due to necessary trade-offs in observation scale, especially in marine systems. By embracing modern mapping technology in ecology, these long-standing constraints can be overcome, leading to an improved understanding of ecosystem dynamics in complex 3D habitats.

Acknowledgements

This work formed part of the SEACAMS and SEACAMS2 projects, part-funded by the European Regional Development Fund (ERDF) through the West Wales and the Valleys Programmes 2007-2013 and 2014-2020, with collaboration from Tidal Lagoon Power, Gloucester, GL2 5RG, UK. AJD was supported by the USDA National Institute of Food and Agriculture, Hatch Formula project accession number 1017848. Aerial imagery was provided under contract by OcuAir, Westbury, BA13 4JT, UK. We would like to thank Michael Roberts and Jonathan King for facilitating the study, and Laura Bush and Alex Vierød for their valuable insights. We thank two anonymous reviewers and Associate Editor Vincent Lecours for their valuable comments that improved the paper.

Author Declaration

All authors have seen and approved the submitted version of the manuscript. All authors have substantially contributed to the work, and all persons entitled to co-authorship have been included. TJB, AJD and GJW conceived and developed the study, TJB, GWS and SR collected the data, TJB processed and analysed the data, TJB, AJD and GJW wrote the manuscript. The manuscript has been submitted solely to *Remote Sensing in Ecology and Conservation* and it has not been published elsewhere, either in part or whole, nor is it in press or under consideration for publication in another journal.

Data accessibility

Data and R code supporting this manuscript are available in Figshare repositories, DOI: 10.6084/m9.figshare.14480709 and DOI: 10.6084/m9.figshare.14480703

References

Anderson, M.J., 2001. A new method for non-parametric multivariate analysis of variance. Austral Ecol. 26, 32–46. https://doi.org/10.1111/j.1442-9993.2001.01070.pp.x

Aston, E.A., Williams, G.J., Green, J.A.M., Davies, A.J., Wedding, L.M., Gove, J.M., Jouffray, J.-B., Jones, T.T., Clark, J., 2019. Scale-dependent spatial patterns in benthic communities around a tropical island seascape. Ecography (Cop.). 42, 578–590. https://doi.org/10.1111/ecog.04097

Ayata, S.-D., Ellien, C., Dumas, F., Dubois, S., Thiébaut, É., 2009. Modelling larval dispersal and settlement of the reef-building polychaete *Sabellaria alveolata*: Role of hydroclimatic processes on the sustainability of biogenic reefs. Cont. Shelf Res. 29, 1605–1623. https://doi.org/10.1016/j.csr.2009.05.002

Bajjouk, T., Jauzein, C., Drumetz, L., Dalla Mura, M., Duval, A., Dubois, S.F., 2020. Hyperspectral and Lidar: Complementary Tools to Identify Benthic Features and Assess the Ecological Status of Sabellaria alveolata Reefs. Front. Mar. Sci. 7, 804. https://doi.org/10.3389/fmars.2020.575218

Barry, J., 1989. Reproductive response of a marine annelid to winter storms: an analog to fire adaptation in plants? Mar. Ecol. Prog. Ser. 54, 99–107. https://doi.org/10.3354/meps054099

Bouma, T.J., van Belzen, J., Balke, T., Zhu, Z., Airoldi, L., Blight, A.J., Davies, A.J., Galvan, C., Hawkins, S.J., Hoggart, S.P.G., Lara, J.L., Losada, I.J., Maza, M., Ondiviela, B., Skov, M.W., Strain, E.M., Thompson, R.C., Yang, S., Zanuttigh, B., Zhang, L., Herman, P.M.J., 2014. Identifying knowledge gaps hampering application of intertidal habitats in coastal protection: Opportunities & steps to take. Coast. Eng. 87, 147–157. https://doi.org/10.1016/j.coastaleng.2013.11.014

Bruschetti, M., 2019. Role of Reef-Building, Ecosystem Engineering Polychaetes in Shallow Water Ecosystems. Diversity 11, 168. https://doi.org/10.3390/d11090168

Bush, L., Balestrini, S., Robins, P., Davies, A., 2015. NRW Evidence Report No 049 - The reproduction and connectivity of *Sabellaria alveolata* reefs in Wales – MAR4REF Bangor University.

Calders, K., Phinn, S., Ferrari, R., Leon, J., Armston, J., Asner, G.P., Disney, M., 2020. 3D Imaging Insights into Forests and Coral Reefs. Trends Ecol. Evol. 35, 6–9. https://doi.org/10.1016/j.tree.2019.10.004

Capa, M., Hutchings, P., Peart, R., 2012. Systematic revision of Sabellariidae (Polychaeta) and their relationships with other polychaetes using morphological and DNA sequence data. Zool. J. Linn. Soc. 164, 245–284. https://doi.org/10.1111/j.1096-3642.2011.00767.x

Chambers, J.Q., Asner, G.P., Morton, D.C., Anderson, L.O., Saatchi, S.S., Espírito-Santo, F.D.B., Palace, M., Souza, C., 2007. Regional ecosystem structure and function: ecological insights from remote sensing of tropical forests. Trends Ecol. Evol. 22, 414–423. https://doi.org/10.1016/j.tree.2007.05.001

Chambers, J.Q., Negron-Juarez, R.I., Marra, D.M., Di Vittorio, A., Tews, J., Roberts, D., Ribeiro, G.H.P.M., Trumbore, S.E., Higuchi, N., 2013. The steady-state mosaic of disturbance and succession across an old-growth Central Amazon forest landscape. Proc. Natl. Acad. Sci. U. S. A. 110, 3949–54. https://doi.org/10.1073/pnas.1202894110

Chappell, J., 1980. Coral morphology, diversity and reef growth. Nature 286, 249–252. https://doi.org/10.1038/286249a0

Chappuis, E., Terradas, M., Cefalì, M.E., Mariani, S., Ballesteros, E., 2014. Vertical zonation is the main distribution pattern of littoral assemblages on rocky shores at a regional scale. Estuar.

Coast. Shelf Sci. 147, 113–122. https://doi.org/10.1016/j.ecss.2014.05.031

Chave, J., 2013. The problem of pattern and scale in ecology: what have we learned in 20 years? Ecol. Lett. 16, 4–16. https://doi.org/10.1111/ele.12048

CloudCompare, 2019. CloudCompare (version 2.11) [GPL software] retrieved from http://www.cloudcompare.org/.

Collin, A., Dubois, S., James, D., Houet, T., 2019. Improving Intertidal Reef Mapping Using UAV Surface, Red Edge, and Near-Infrared Data. Drones 3, 67. https://doi.org/10.3390/drones3030067

Collin, A., Dubois, S., Ramambason, C., Etienne, S., 2018. Very high-resolution mapping of emerging biogenic reefs using airborne optical imagery and neural network: the honeycomb worm (*Sabellaria alveolata*) case study. Int. J. Remote Sens. 39, 5660–5675. https://doi.org/10.1080/01431161.2018.1484964

Connell, J.H., 1978. Diversity in Tropical Rain Forests and Coral Reefs. Science 199, 1302–1310.

Connell, J.H., 1972. Community Interactions on Marine Rocky Intertidal Shores. Annu. Rev. Ecol. Syst. 3, 169–192. https://doi.org/10.1146/annurev.es.03.110172.001125

Crisp, D.J., 1964. The Effects of the Severe Winter of 1962-63 on Marine Life in Britain. J. Anim. Ecol. 33, 165. https://doi.org/10.2307/2355

Curd, A., Pernet, F., Corporeau, C., Delisle, L., Firth, L.B., Nunes, F.L.D., Dubois, S.F., 2019. Connecting organic to mineral: How the physiological state of an ecosystem-engineer is linked to its habitat structure. Ecol. Indic. 98, 49–60. https://doi.org/10.1016/J.ECOLIND.2018.10.044

D'Urban Jackson, T., Williams, G.J., Walker-Springett, G., Davies, A.J., 2020. Three-dimensional digital mapping of ecosystems: A new era in spatial ecology. Proc. R. Soc. B Biol. Sci. 287, 1–10. https://doi.org/10.1098/rspb.2019.2383

Denny, M.W., Helmuth, B., Leonard, G.H., Harley, C.D.G., Hunt, L.J.H., Nelson, E.K., 2004. Quantifying scale in ecology: Lessons from a wave-swept shore. Ecol. Monogr. 74, 513–532. https://doi.org/10.1890/03-4043

Dubois, S., Comtet, T., Retiére, C., Thiébaut, É., 2007. Distribution and retention of *Sabellaria alveolata* larvae (Polychaeta: Sabellariidae) in the Bay of Mont-Saint-Michel, France. Mar. Ecol. Prog. Ser. 346, 243–254. https://doi.org/10.3354/meps07011

Dubois, S., Retiere, C., Olivier, F., 2002. Biodiversity associated with *Sabellaria alveolata* (Polychaeta: Sabellariidae) reefs: effects of human disturbances. J. Mar. Biol. Assoc. UK 82, 817–826. https://doi.org/10.1017/S0025315402006185

Edwards, C.B., Eynaud, Y., Williams, G.J., Pedersen, N.E., Zgliczynski, B.J., Gleason, A.C.R., Smith, J.E., Sandin, S.A., 2017. Large-area imaging reveals biologically driven non-random spatial patterns of corals at a remote reef. Coral Reefs 36, 1291–1305. https://doi.org/10.1007/s00338-017-1624-3

Firth, L.B., Mieszkowska, N., Grant, L.M., Bush, L.E., Davies, A.J., Frost, M.T., Moschella, P.S., Burrows, M.T., Cunningham, P.N., Dye, S.R., Hawkins, S.J., 2015. Historical comparisons reveal multiple drivers of decadal change of an ecosystem engineer at the range edge. Ecol. Evol. 5, 3210–3222. https://doi.org/10.1002/ece3.1556

Ford, H. V., Gove, J.M., Davies, A.J., Graham, N.A.J., Healey, J.R., Conklin, E.J., Williams, G.J., 2020. Spatial scaling properties of coral reef benthic communities. Ecography (Cop.). ecog.05331. https://doi.org/10.1111/ecog.05331

Godet, L., Fournier, J., Jaffré, M., Desroy, N., 2011. Influence of stability and fragmentation of a worm-reef on benthic macrofauna. Estuar. Coast. Shelf Sci. 92, 472–479.

https://doi.org/10.1016/j.ecss.2011.02.003

Graham, N.A.J., Jennings, S., MacNeil, M.A., Mouillot, D., Wilson, S.K., 2015. Predicting climate-driven regime shifts versus rebound potential in coral reefs. Nature 518, 94–97. https://doi.org/10.1038/nature14140

Graham, N.A.J., Nash, K.L., 2013. The importance of structural complexity in coral reef ecosystems. Coral Reefs 32, 315–326. https://doi.org/10.1007/s00338-012-0984-y

Graler, B., Pebesma, E., Heuvelink, G., 2016. Spatio-Temporal Interpolation using gstat. Wp 1–20.

Gringarten, E., Deutsch, C. V, 2001. Teacher's aide: Variogram interpretation and modeling. Math. Geol. 33, 507–534. https://doi.org/10.1023/A:1011093014141

Gruet, Y., 1986. Spatio-temporal Changes of Sabellarian Reefs Built by the Sedentary Polychaete *Sabellaria alveolata* (Linné). Mar. Ecol. 7, 303–319. https://doi.org/10.1111/j.1439-0485.1986.tb00166.x

Guichard, F., Halpin, P.M., Allison, G.W., Lubchenco, J., Menge, B.A., 2003. Mussel Disturbance Dynamics: Signatures of Oceanographic Forcing from Local Interactions. Am. Nat. 161, 889–904. https://doi.org/10.1086/375300

Holt, T., Rees, E., Hawkins, S., Seed, R., 1998. Biogenic Reefs (volume IX). An overview of dynamic and sensitivity characteristics for conservation management of marine SACs. Scottish Association for Marine Science (UK Marine SACs Project).

Horne, J.K., Schneider, D.C., 1995. Spatial Variance in Ecology. Oikos 74, 18. https://doi.org/10.2307/3545670

Jenkins, C., Eggleton, J., Barry, J., O'Connor, J., 2018. Advances in assessing Sabellaria spinulosa reefs for ongoing monitoring. Ecol. Evol. 8, 7673–7687. https://doi.org/10.1002/ece3.4292

Jones, C.G., Lawton, J.H., Shachak, M., 1994. Organisms as Ecosystem Engineers. Oikos 69, 373. https://doi.org/10.2307/3545850

Kaiser, M.S., Speckman, P.L., Jones, J.R., 1994. Statistical models for limiting nutrient relations in inland waters. J. Am. Stat. Assoc. 89, 410–423. https://doi.org/10.1080/01621459.1994.10476763

Kaufman, L., Rousseeuw, P.J., 1990. Finding Groups in Data, Finding Groups in Data: An Introduction to Cluster Analysis, Wiley Series in Probability and Statistics. John Wiley & Sons, Inc., Hoboken, NJ, USA. https://doi.org/10.1002/9780470316801

Klausmeier, C.A., 1999. Regular and irregular patterns in semiarid vegetation. Science 284, 1826–1828. https://doi.org/10.1126/science.284.5421.1826

Koenker, R., 2020. quantreg: Quantile Regression. R package version 5.83. https://CRAN.R-project.org/package=quantreg.

La Porta, B., Nicoletti, L., 2009. *Sabellaria alveolata* (Linnaeus) reefs in the central Tyrrhenian Sea (Italy) and associated polychaete fauna. Zoosymposia 2, 527–536. https://doi.org/10.11646/zoosymposia.2.1.36

Landres, P.B., Morgan, P., Swanson, F.J., 1999. Overview of the use of natural variability concepts in managing ecological systems. Ecol. Appl. 9, 1179–1188. https://doi.org/10.1890/1051-0761(1999)009[1179:OOTUON]2.0.CO;2

Le Cam, J.-B., Fournier, J., Etienne, S., Couden, J., 2011. The strength of biogenic sand reefs: Visco-elastic behaviour of cement secreted by the tube building polychaete *Sabellaria alveolata*, Linnaeus, 1767. Estuar. Coast. Shelf Sci. 91, 333–339. https://doi.org/10.1016/j.ecss.2010.10.036

611 Lecornu, B., Schlund, E., Basuyaux, O., Cantat, O., Dauvin, J.-C.C., 2016. Dynamics (from 2010-
612 2011 to 2014) of *Sabellaria alveolata* reefs on the western coast of Cotentin (English Channel,
613 France). Reg. Stud. Mar. Sci. 8, 157–169. https://doi.org/10.1016/j.rsma.2016.07.004

614 Lecours, V., Devillers, R., Schneider, D.C., Lucieer, V.L., Brown, C.J., Edinger, E.N., 2015. Spatial
615 scale and geographic context in benthic habitat mapping: Review and future directions. Mar.
616 Ecol. Prog. Ser. 535, 259–284. https://doi.org/10.3354/meps11378

617 Legendre, P., Fortin, M.J., 1989. Spatial pattern and ecological analysis. Vegetatio 80, 107–138.
618 https://doi.org/10.1007/BF00048036

619 Lepczyk, C.A., Wedding, L.M., Asner, G.P., Pittman, S.J., Goulden, T., Linderman, M.A., Gang, J.,
620 Wright, R., 2021. Advancing Landscape and Seascape Ecology from a 2D to a 3D Science.
621 Bioscience. https://doi.org/10.1093/biosci/biab001

622 Levin, S.A., 1992. The Problem of Pattern and Scale in Ecology: The Robert H. MacArthur Award
623 Lecture Author(s): Simon A. Levin Source: Ecology 73, 1943–1967.
624 https://doi.org/doi:10.2307/1941447

625 Liu, Q.-X., Herman, P.M.J., Mooij, W.M., Huisman, J., Scheffer, M., Olff, H., van de Koppel, J.,
626 2014. Pattern formation at multiple spatial scales drives the resilience of mussel bed ecosystems.
627 Nat. Commun. 5, 5234. https://doi.org/10.1038/ncomms6234

628 Lowe, R.J., Falter, J.L., Bandet, M.D., Pawlak, G., Atkinson, M.J., Monismith, S.G., Koseff, J.R.,
629 2005. Spectral wave dissipation over a barrier reef. J. Geophys. Res. C Ocean. 110, 1–16.
630 https://doi.org/10.1029/2004JC002711

631 Maechler, M., Rousseeuw, P.J., Struyf, A., Hubert, M., Hornik, K., 2019. cluster: Cluster Analysis
632 Basics and Extensions. R package version 2.1.0.

633 Odum, E.P., 1969. The Strategy of Ecosystem Development. Science 164, 262–270.

634 Pebesma, E.J., 2004. Multivariable geostatistics in {S}: the gstat package. Comput. Geosci. 30, 683–
635 691.

636 Pennings, S.C., Callaway, R.M., 1992. Salt marsh plant zonation: the relative importance of
637 competition and physical factors. Ecology 73, 681–690. https://doi.org/10.2307/1940774

638 Perry, G.L.W., 2002. Landscapes, space and equilibrium: Shifting viewpoints. Prog. Phys. Geogr. 26,
639 339–359. https://doi.org/10.1191/0309133302pp341ra

640 Peterson, R.A., Cavanaugh, J.E., 2020. Ordered quantile normalization: a semiparametric
641 transformation built for the cross-validation era. J. Appl. Stat. 47, 2312–2327.
642 https://doi.org/10.1080/02664763.2019.1630372

643 R Core Team, 2020. R: A language and environment for statistical computing. R Foundation for
644 Statistical Computing, Vienna, Austria. URL https://www.R-project.org/.

645 Rodriguez, A.B., Fodrie, F.J., Ridge, J.T., Lindquist, N.L., Theuerkauf, E.J., Coleman, S.E.,
646 Grabowski, J.H., Brodeur, M.C., Gittman, R.K., Keller, D. a., Kenworthy, M.D., 2014. Oyster
647 reefs can outpace sea-level rise. Nat. Clim. Chang. 4, 493–497.
648 https://doi.org/10.1038/nclimate2216

649 Safriel, U.N., Ben-Eliahu, M.N., 1991. The influence of habitat structure and environmental stability
650 on the species diversity of polychaetes in vermetid reefs, in: Bell, S.S., McCoy, E.D.,
651 Mushinsky, H.R. (Eds.), Habitat Structure. Chapman & Hall/CRC, London, pp. 349–368.
652 https://doi.org/10.1007/978-94-011-3076-9

653 Scheffers, B.R., Edwards, D.P., Diesmos, A., Williams, S.E., Evans, T.A., 2014. Microhabitats reduce
654 animal's exposure to climate extremes. Glob. Chang. Biol. 20, 495–503.
655 https://doi.org/10.1111/gcb.12439

Stevenson, A., Mitchell, F.J.G., Davies, J.S., 2015. Predation has no competition: factors influencing space and resource use by echinoids in deep-sea coral habitats, as evidenced by continuous video transects. Mar. Ecol. 36, 1454–1467. https://doi.org/10.1111/maec.12245

Stone, R., Callaway, R., Bull, J.C., 2019. Are biodiversity offsetting targets of ecological equivalence feasible for biogenic reef habitats? Ocean Coast. Manag. 177, 97–111. https://doi.org/10.1016/j.ocecoaman.2019.04.003

Turner, M.G., Romme, W.H., Gardner, R.H., O'Neill, R. V., Kratz, T.K., 1993. A revised concept of landscape equilibrium: Disturbance and stability on scaled landscapes. Landsc. Ecol. 8, 213–227. https://doi.org/10.1007/BF00125352

Underwood, A.J., Chapman, M.G., Connell, S.D., 2000. Observations in ecology: You can't make progress on processes without understanding the patterns. J. Exp. Mar. Bio. Ecol. 250, 97–115. https://doi.org/10.1016/S0022-0981(00)00181-7

Urbina-Barreto, I., Chiroleu, F., Pinel, R., Fréchon, L., Mahamadaly, V., Elise, S., Kulbicki, M., Quod, J.P., Dutrieux, E., Garnier, R., Henrich Bruggemann, J., Penin, L., Adjeroud, M., 2021. Quantifying the shelter capacity of coral reefs using photogrammetric 3D modeling: From colonies to reefscapes. Ecol. Indic. 121, 107151. https://doi.org/10.1016/j.ecolind.2020.107151

Van De Koppel, J., Gascoigne, J.C., Theraulaz, G., Rietkerk, M., Mooij, W.M., Herman, P.M.J., 2008. Experimental evidence for spatial self-organization and its emergent effects in mussel bed ecosystems. Science 322, 739–742. https://doi.org/10.1126/science.1163952

Ventura, D., Dubois, S.F., Bonifazi, A., Jona Lasinio, G., Seminara, M., Gravina, M.F., Ardizzone, G., 2020. Integration of close-range underwater photogrammetry with inspection and mesh processing software: a novel approach for quantifying ecological dynamics of temperate biogenic reefs. Remote Sens. Ecol. Conserv. rse2.178. https://doi.org/10.1002/rse2.178

Vierling, K.T., Vierling, L.A., Gould, W.A., Martinuzzi, S., Clawges, R.M., 2008. Lidar: Shedding new light on habitat characterization and modeling. Front. Ecol. Environ. 6, 90–98. https://doi.org/10.1890/070001

Warfe, D.M., Barmuta, L.A., Wotherspoon, S., 2008. Quantifying habitat structure: surface convolution and living space for species in complex environments. Oikos 117, 1764–1773. https://doi.org/10.1111/j.1600-0706.2008.16836.x

Wedding, L., Lepczyk, C., Pittman, S., Friedlander, A., Jorgensen, S., 2011. Quantifying seascape structure: extending terrestrial spatial pattern metrics to the marine realm. Mar. Ecol. Prog. Ser. 427, 219–232. https://doi.org/10.3354/meps09119

Wedding, L.M., Jorgensen, S., Lepczyk, C.A., Friedlander, A.M., 2019. Remote sensing of three-dimensional coral reef structure enhances predictive modeling of fish assemblages. Remote Sens. Ecol. Conserv. 5, 150–159. https://doi.org/10.1002/rse2.115

Wiens, J.A., 1989. Spatial Scaling in Ecology. Funct. Ecol. 3, 385. https://doi.org/10.2307/2389612

Williams, G.J., Graham, N.A.J., Jouffray, J.B., Norström, A. V., Nyström, M., Gove, J.M., Heenan, A., Wedding, L.M., 2019. Coral reef ecology in the Anthropocene. Funct. Ecol. 33, 1014–1022. https://doi.org/10.1111/1365-2435.13290

Wilson, D.P., 1971. Sabellaria Colonies at Duckpool, North Cornwall. J. Mar. Biol. Assoc. UK 51, 509–580.

Woodhead, A.J., Hicks, C.C., Norström, A. V., Williams, G.J., Graham, N.A.J., 2019. Coral reef ecosystem services in the Anthropocene. Funct. Ecol. 33, 1023–1034. https://doi.org/10.1111/1365-2435.13331

Figures

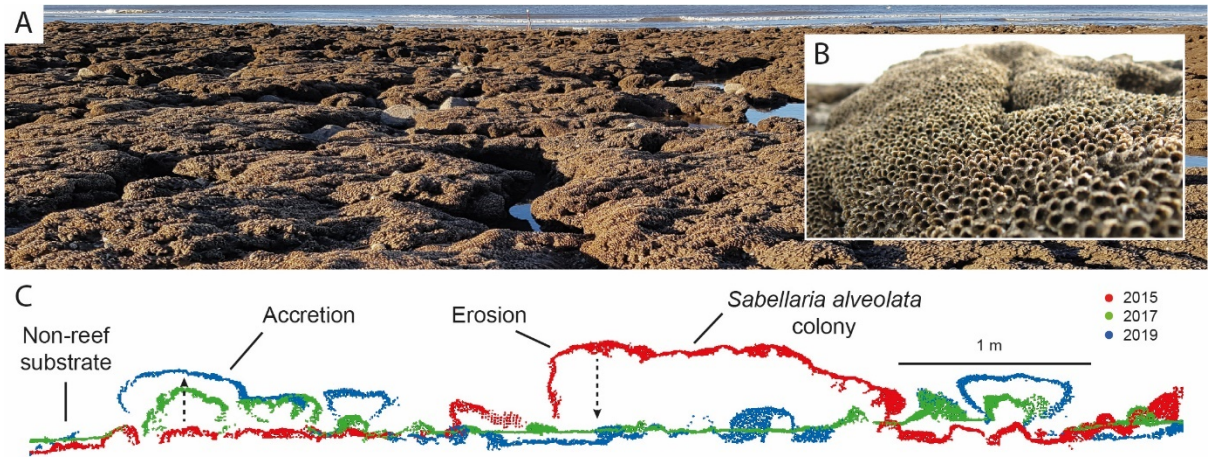

Figure 1. A) *Sabellaria alveolata* biogenic reef habitat comprises aggregations of sediment tubes in colonies that emerge above a hard, non-reef substrate. B) Close-up image of a prograding colony surface showing dense tube openings of ~5 mm diameter. C) Cross section of 3D terrestrial laser scan point cloud data from 3 years, demonstrating the detailed information about spatial and temporal dynamics in habitat structure that can be captured using modern 3D mapping technology. Reef colonies accrete upwards and outwards from the non-reef substrate in characteristic mushroom-like hummocks that coalesce into platforms. Erosion of reef colonies is often rapid and catastrophic.

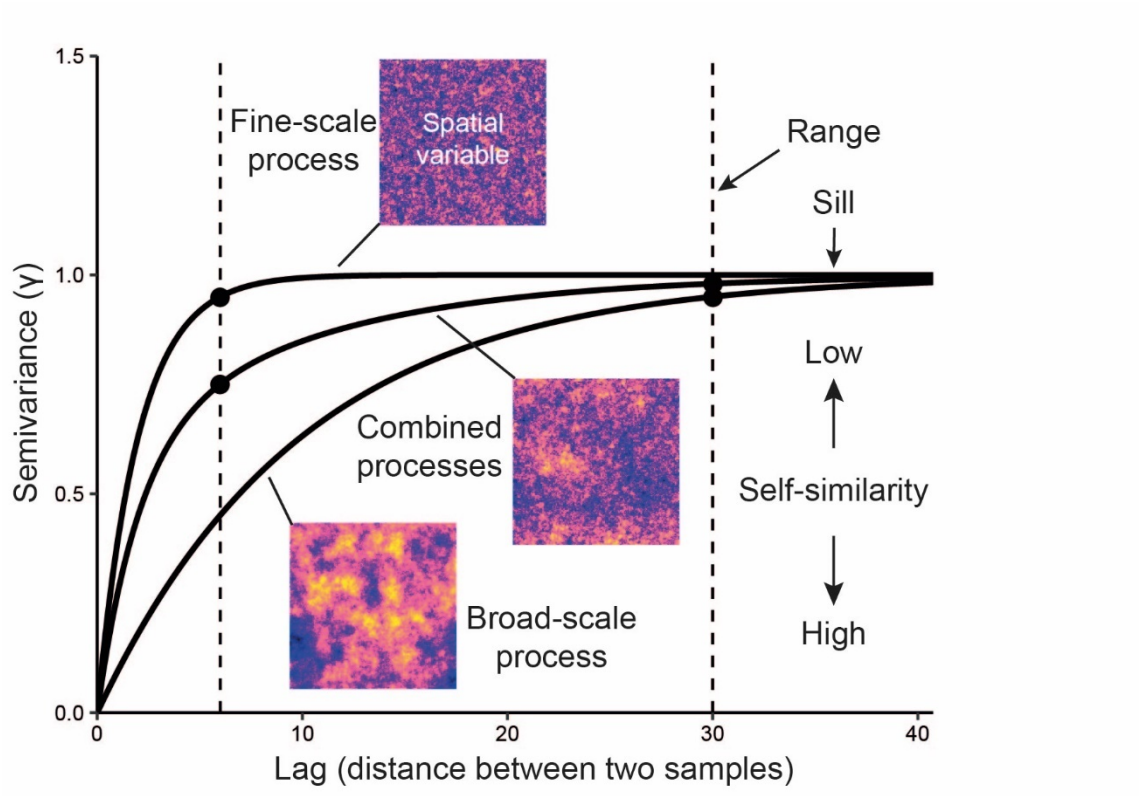

Figure 2. Interpreting spatial patterns in processes that generate spatial variables using variography. Variograms visualise spatial self-similarity, or autocorrelation, in a variable by plotting semivariance (γ) against lag, the distance between two samples. As lag increases samples become less similar (higher γ) until a plateau (sill) is reached at a distance (range), beyond which sample values are not autocorrelated. Here we show three simulated examples of a variable generated with different processes, and their respective variograms. Top: a fine-scale process generates a variable that is autocorrelated only over short distances, so the range (point and dashed line) is small. Bottom: a broad-scale process generates a variable that is autocorrelated over longer distances, producing a variogram with a larger range. Middle: the fine- and broad- scale processes have been added together, producing a variable with both short- and long-distance autocorrelation, generating a nested variogram with two ranges.

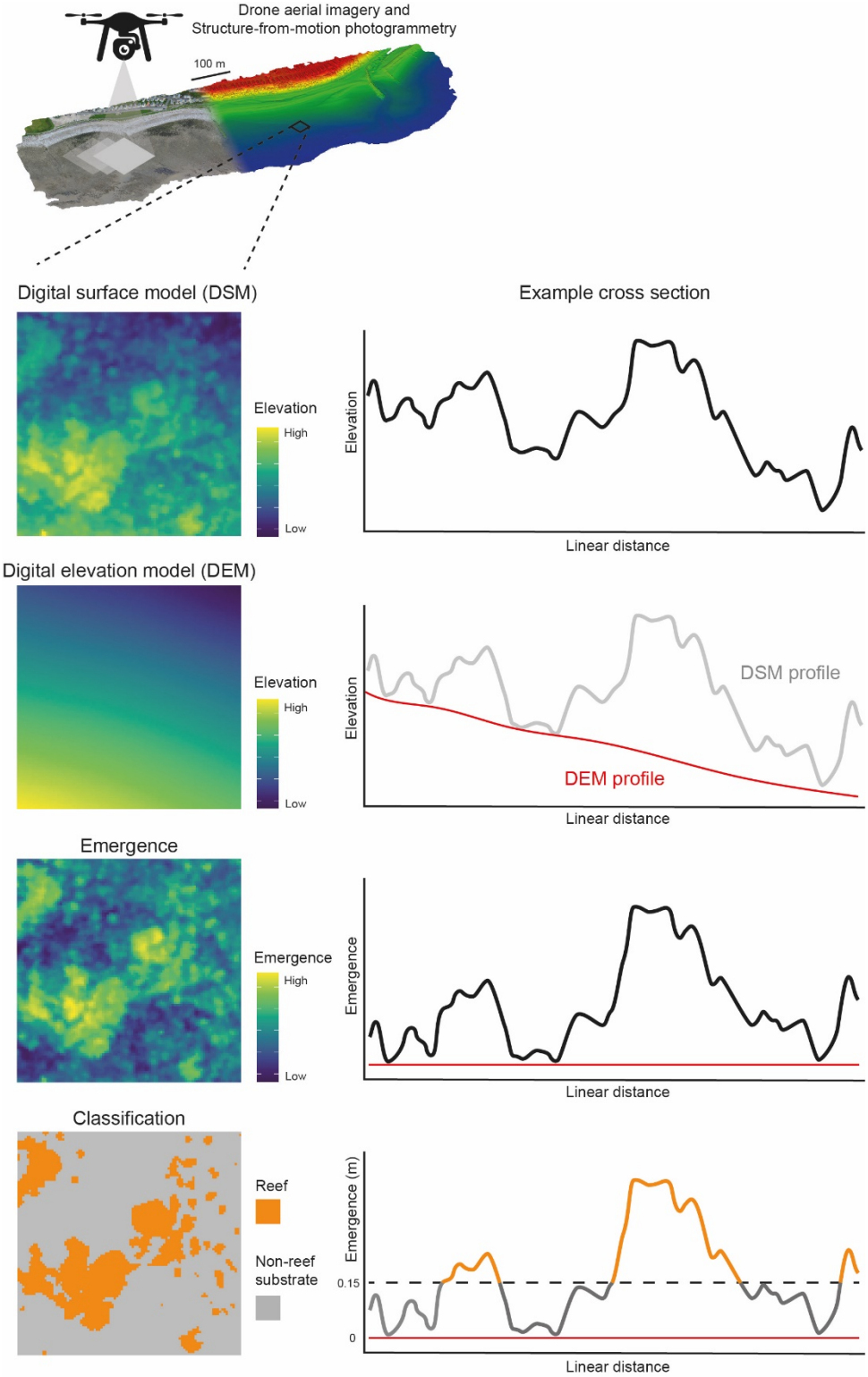

Figure 3: Data processing method used to classify habitat-scale digital surface models (DSMs) as reef or non-reef substrate. We generated 0.1 m XY resolution DSMs using drone aerial imagery and structure-from-motion photogrammetry. From the DSM we generated a digital elevation model (DEM) representing the ground level at the same resolution by interpolating between the lowest point in each square of a 2 m grid. We calculated emergence by subtracting the DEM from the DSM elevation. Finally, within the known reef area (Fig. 5A) we used a binary classification of reef (≥0.15 m emergence) and non-reef substrate (<0.15 m emergence).

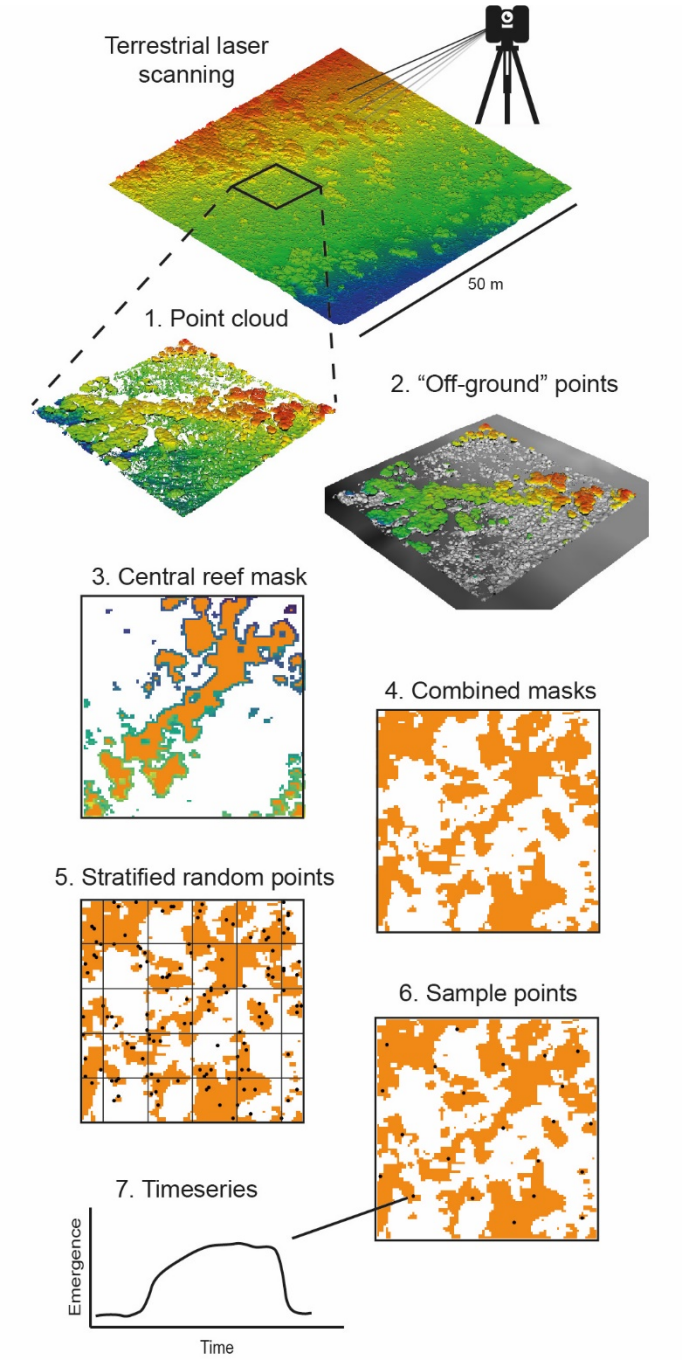

Figure 4. Data processing method used to sample reef emergence through time at independent reef locations within a 50 x 50 m plot mapped using terrestrial laser scanning at 6-month intervals over 5 years (Supporting information). 1) Example section of 3D point cloud data. 2) We used a cloth simulation filter to generate a digital elevation model (DEM) for each time point and retained only points ≥0.2 m above the DEM. 3) We generated a digital surface model (DSM, 0.1 m XY resolution) of mean point elevation, then used the DSM to generate a mask that removed low point density cells, isolated cells, and colony edges. 4) We combined the masks from all time points. 5) We used a 2 m grid to generate spatially stratified random points (5 points per strata). 6) We randomly selected one point per strata with a minimum spacing of 1.5 m to generate our sample point locations. 7) At each sample location we calculated a timeseries of emergence by subtracting the elevation of a common digital elevation model representing the ground level from the DSM for each time point (Fig. 7).

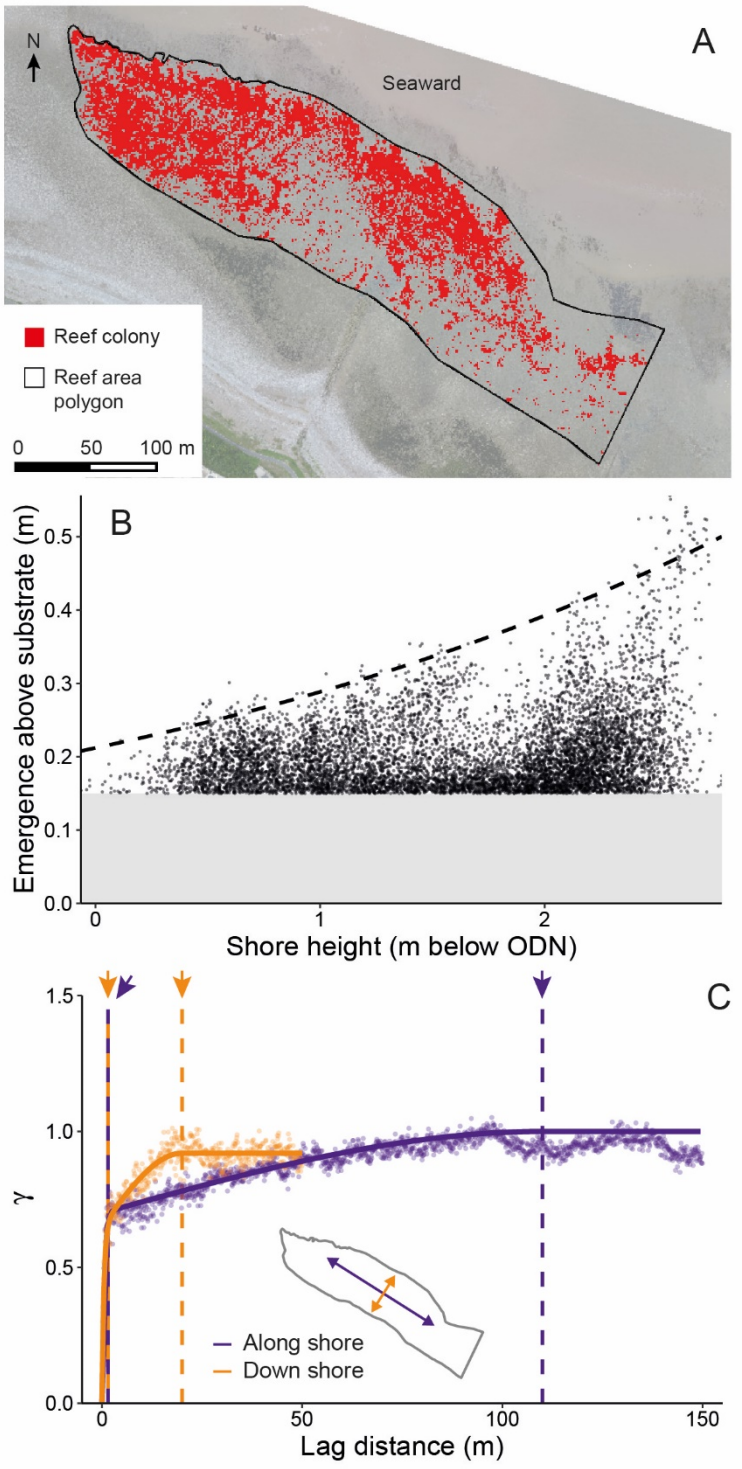

Figure 5. A) The foreshore at Llanddulas, Wales, UK. Habitat-scale 3D structure data were analysed within a 36,363 m^2 reef area polygon digitised from an aerial imagery orthomosaic. Presence of emergent reef is shown at 1 m XY resolution. B) Maximum reef colony emergence increases lower down the shore. The reef colonies that we analysed had a minimum emergence of 0.15 m. C) Reef colony emergence was spatially autocorrelated over short distances (1.5 m) both along the shore (purple) and down the shore (orange), ranges indicated by left-most vertical lines and arrows. There was a secondary autocorrelation structure that had a longer range (110 m) in the along shore direction compared to down the shore (20 m), ranges shown by right-most vertical lines and arrows.

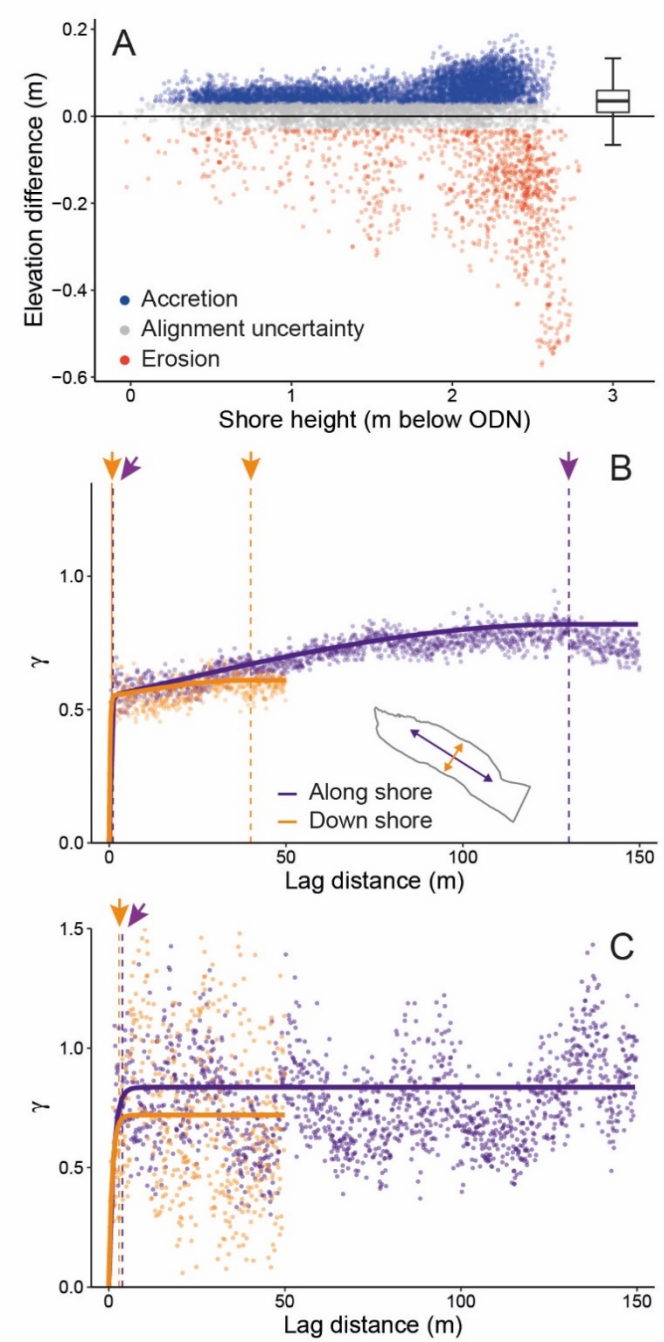

758

759 **Figure 6.** Spatial variation in *S. alveolata* reef elevation changes from April 2018 to April 2019
760 within the reef area (Fig. 5A). A) Both positive and negative elevation changes increased towards the
761 lower shore. Samples showing positive changes (blue) were greater in number than those with
762 negative change (red), but the larger average magnitude of negative changes resulted in little change
763 in overall elevation, shown by the boxplot of all samples crossing 0. Grey points represent samples
764 with changes within the alignment uncertainty estimate of ±0.03 m. B) Variogram showing spatial
765 autocorrelation scales of positive elevation changes (accretion) after accounting for trend (Supporting
766 information table S2). The majority of spatial autocorrelation is explained by a short range (0.75 –
767 1.05 m) structure (left-most vertical lines and arrows), with a secondary structure showing a longer
768 range (130 m) in the alongshore orientation compared to down the shore (30 m). C) Variogram
769 showing spatial scales of negative elevation changes (erosion) after accounting for trend (Supporting
770 information table S2). Spatial autocorrelation only occurs up to a short range (2.9 – 3.84 m, vertical
771 lines and arrows).

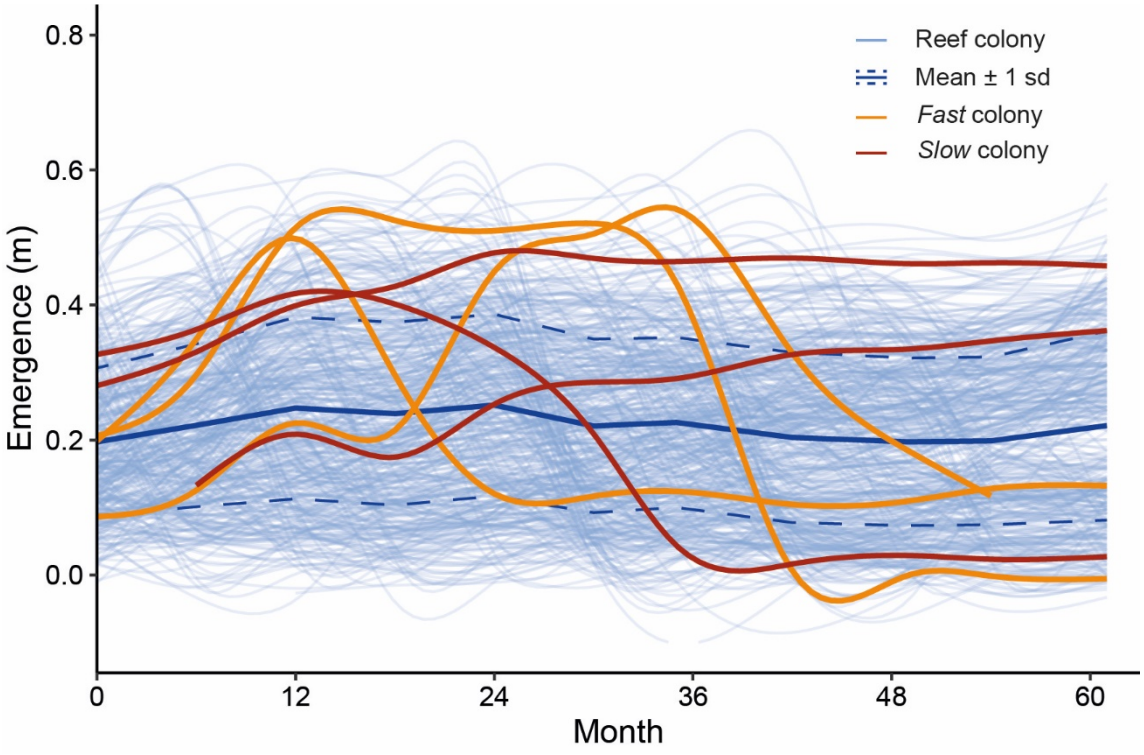

Figure 7. Colony-scale variation balances out to produce plot-scale stability in *S. alveolata* reef habitat structure over several years. Emergence was measured at 454 stratified random, spatially independent sample locations in a 2,500 m^2 plot in autumn and spring each year from September 2014 (month 0) to October 2019 (month 61). Thin blue lines show individual sample timeseries. Bold blue line and dashed lines show the mean ± 1 sd emergence of all samples. Six example sample timeseries' are highlighted to show the diversity of fine-scale dynamics in reef accretion and loss over time, clustered into two groups: *fast* colonies with rapid accretion and short persistence (orange) and *slow* colonies with slower accretion and longer persistence (red).